Virus-specific CD8+ T cells accumulate near sensory nerve endings in genital skin during subclinical HSV-2 reactivation

Jia Zhu,[1,6] David M. Koelle,[1,2,4,6,9] Jianhong Cao,[7] Julio Vazquez,[8] Meei Li Huang,[1,6] Florian Hladik,[2,5,6] Anna Wald,[1,2,3,6] and Lawrence Corey[1,2,4,6]

[1]Department of Laboratory Medicine, [2]Department of Medicine, [3]Department of Epidemiology, [4]Department of Pathobiology, and [5]Department of Obstetrics and Gynecology, University of Washington, Seattle, WA 98195
[6]Infectious Diseases Program, [7]Immune Monitoring Lab, and [8]Scientific Imaging, Fred Hutchinson Cancer Research Center, Seattle, WA 98109
[9]Benaroya Research Institute, Seattle, WA 98104

Cytotoxic CD8+ T cells play a critical role in controlling herpes simplex virus (HSV) infection and reactivation. However, little is known about the spatiotemporal dynamics of CD8+ T cells during HSV lesion evolution or about their involvement in immune surveillance after lesion resolution. Using quantum dot–conjugated peptide–major histocompatibility complex multimers, we investigated the in vivo localization of HSV-2–specific CD8+ T cells in sequential biopsies of human genital skin during acute, resolving, and healed stages of HSV-2 reactivation. Our studies revealed that functionally active CD8+ T cells selectively infiltrated to the site of viral reactivation. After lesion healing in concert with complete reepithelialization and loss of HSV DNA from skin biopsies, HSV-2–specific CD8+ T cells persisted for more than two months at the dermal–epidermal junction, adjacent to peripheral nerve endings. In two out of the six sequentially studied individuals, HSV-2 DNA reappeared in clinically and histologically normal–appearing skin. Detection of viral DNA was accompanied by increased numbers of both HSV-specific and total CD8+ T cells in the dermis. These findings indicate that the frequency and clinical course of HSV-2 reactivation in humans is influenced by virus-specific CD8+ T cells that persist in peripheral mucosa and genital skin after resolution of herpes lesions.

CORRESPONDENCE
Lawrence Corey:
lcorey@u.washington.edu

Abbreviations used: NCAM, neural cell adhesion molecule; Qdot, quantum dot; Qdot multimer, Qdot-conjugated peptide–MHC multimer.

Several lines of evidence support the importance of CD8+ T cells in limiting HSV reactivation from latently infected ganglia and in controlling lytic mucocutaneous infection. Patients with iatrogenic immune suppression and hereditary or acquired immunodeficiency experience both more frequent reactivation and prolonged symptomatic episodes of infection (1–3). In mice, HSV-1–specific T cells have been demonstrated in latently infected neural ganglia, and depletion or neutralization of these cells from the ganglionic neural tissue is associated with reactivation of virus from neural tissue in an ex vivo explant model (4, 5). In humans, CD8+ T cells have been shown to infiltrate genital lesions, and the clearance of HSV-2 from genital herpes lesions is associated with the influx of HSV-specific CD8+ T cells (6–9). However, little is known of the spatial distribution of HSV-specific T cells with respect to HSV-infected cells, their persistence after lesion resolution, and the relative importance of host immunity in the ganglion versus peripheral mucosal areas in containing viral reactivation.

In situ staining of pathogen-specific CD8+ T cells has been demonstrated using antigen-specific tetramers (10, 11). This technology has been used to evaluate compartmentalized immune responses to a variety of infections that stimulate high frequencies of pathogen-specific T cells (12, 13). HSV infections of humans offer challenges for such technology, as the frequency of total HSV-specific CD8+ T cell responses in PBMCs are much lower than in HIV or EBV infection (14–16), and human skin has much higher autofluorescence than lymphoid tissue (17–19). Quantum dots (Qdots) are fluorescent

The online version of this article contains supplemental material.

The Journal of Experimental Medicine

nanoscaled crystalline probes that offer several advantages for cellular labeling and imaging (20–22). In this study, we describe the synthesis of Qdot-conjugated peptide–MHC multimers (Qdot multimers), which provide higher sensitivity and photostability than conventional tetramers (23). We used these reagents to demonstrate the in vivo persistence of HSV-2–specific $CD8^+$ T cells in genital skin after disease resolution, their location contiguous to peripheral nerve endings at the dermal–epidermal junction, and their role in containing the formation of lesions caused by reactivated virus. Our data suggest that for HSV-2, containment by virus-specific $CD8^+$ T cells in the periphery appears to be an important, if not the predominant, means by which the host limits HSV-2 at mucosal surfaces.

RESULTS

To study the spatiotemporal distribution of HSV-2–specific $CD8^+$ T cells during the evolution of HSV-2 reactivation, serial 3-mm punch biopsies from six HSV-2 seropositive, HIV seronegative subjects with recurrent genital herpes were obtained. Patients were selected from a cohort of persons who participated in prior studies and who had defined $CD8^+$ T cell responses to HSV-2 (8,14). Patients underwent from two to seven separate biopsies over the course of study (Table I). Qdot multimers recognizing peptide epitopes encoded by HSV-2 *UL26*, *UL27*, *UL46*, *UL47*, and *UL49* genes were synthesized, and in situ staining for HSV-2–specific $CD8^+$ T cells was conducted.

CD8 cytolytic activity at the site of herpes recurrence

During the acute phase of genital recurrence, productive HSV-2 viral replication was associated with disruption of the epidermal layer (Fig. 1 a). Immune cell infiltration was massive at the site of infection and differed markedly from that observed in biopsies taken at the same time from distant skin sites (Fig. 1 a). $CD8^+$ T cells were detected both below and within the HSV-2–infected epidermis (Video 1, available at http://www.jem.org/cgi/content/full/jem.20061792/DC1); three-dimensional modeling constructed from confocal images of the late ulcer/early crust stage (Fig. 1 b) revealed cell-to-cell interactions between $CD8^+$ T lymphocytes and the HSV-2–infected epidermal keratinocytes. The presence of multiple junctions between $CD8^+$ T cells and HSV-2–infected keratinocytes is consistent with the formation of immunological synapses between antigen-specific $CD8^+$ T cells and their targets in vivo (Video 2). To demonstrate the functional competence of these $CD8^+$ T cells, lymphocytes were recovered from recurrent genital lesions biopsied at the time of HSV-2 culture conversion from positive to negative. The lymphocytes were expanded and examined for cytolytic function by chromium release assays, as previously described (9). $CD4^+$ $CD8^-$ and $CD4^-$ $CD8^+$ T lymphocytes and $CD3^-$ $CD56^+$ NK cells were the three main subpopulations detected after expansion (Fig. 1 c). HLA class I–restricted, HSV-2 antigen–specific cytolytic activity of $CD8^+$ T cells was clearly present both at bulk culture and selected T cell levels (Fig. 1 c), indicating that $CD8^+$ cytolytic T lymphocytes specific for HSV-2 contribute to the resolution of lesions in patients with genital herpes.

Qdot multimers

Based on previous work defining the HSV-2–specific epitopes and immunodominant responses restricted by HLA A*0101, A*0201, and B*0702 alleles (8, 24), peptides encoded by the HSV-2 *UL26*, *UL27*, *UL46*, *UL47*, and *UL49* genes were used to synthesize Qdot 655–conjugated multimers (see Materials and methods). Qdot 655 conjugates were constructed to average between seven and eight streptavidin molecules covalently attached to each Qdot particle, thus binding up to 32 peptide–MHC monomers under saturated condition (Fig. 2 a). The photostability of the Qdot multimer allowed high quality confocal laser scanning, including detailed imaging of TCR molecules on the cell surface (Fig. 2 b and Video 3, available at http://www.jem.org/cgi/content/full/jem.20061792/DC1). The Qdot 655 multimers exhibited similar specificity but had higher signal

Table I. Clinical history of genital herpes and time of genital lesion biopsies studied

Subjects	P1	P2	P3	P4	P5	P6
HSV serology	1 and 2	2	1 and 2	1 and 2	1 and 2	2
Age/gender	46/female	58/male	44/female	54/female	42/female	41/female
No. years with HSV-2	28	25	18	16	22	20
Lesion site	labia	buttock	buttock	buttock	perianal	buttock
Stage of genital lesion at time of biopsy	ulcer crust healed 2 wk p.h. 4 wk p.h. 6 wk p.h. 8 wk p.h.	pustule crust 2 wk p.h. 4 wk p.h. 6 wk p.h. 8 wk p.h.	pustule crust 2 wk p.h. 4 wk p.h. 8 wk p.h.	crust 2 wk p.h. 6 wk p.h.	ulcer 2 wk p.h. 6 wk p.h.	crust 4 wk p.h.
HLA type	A01, 26; B07, 08	A01, 02; B08, 45	A11, 29; B07, 41	A02, 23; B49, 60	A68; B35, 44	A01, 02; B08, 57

p.h., post-healing of the lesion (skin epithelialized).

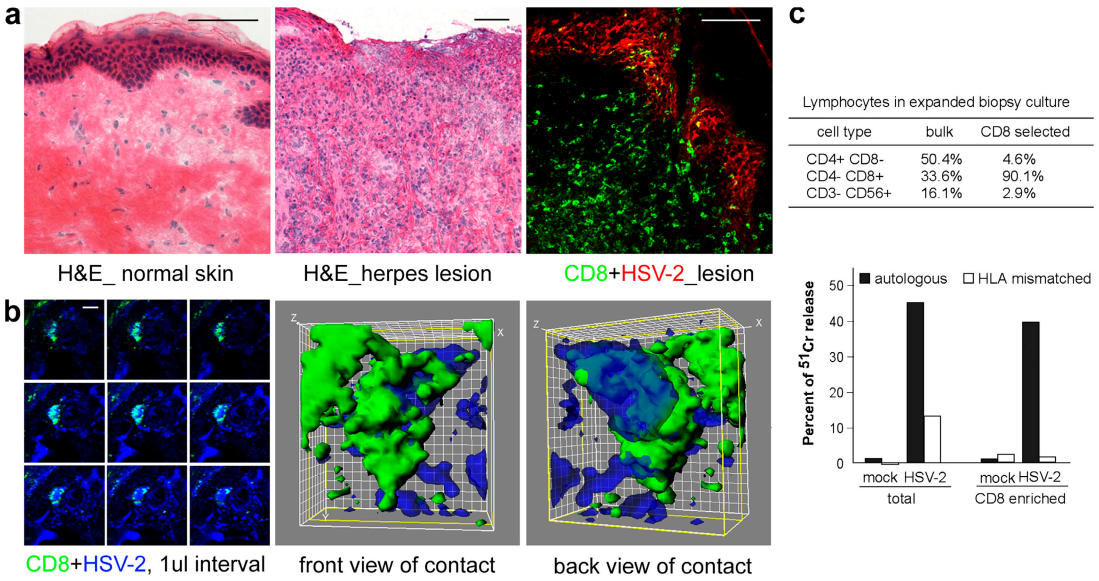

Figure 1. Spatial and functional CD8⁺ CTL activity during an acute genital herpetic lesion. (a) Hematoxylin and eosin staining of normal arm (left) and lesional skin (middle). Immunofluorescence staining (right) for CD8⁺ cells (green) and HSV-2–infected cells (red). (b) Confocal image of CD8⁺ and HSV-2–infected cells in an acute lesion. Montages of a CD8⁺ cell (green) in proximity to HSV-2–infected cells (blue) were displayed at 1-μm intervals (left). (middle and right) The 0° (front) and 180° (back) views of a three-dimensional rendering of the interactions. (c) HSV-2–specific CD8 cytolytic activity as measured by chromium release in lymphocytes cultured from a lesion biopsy 5 d after onset, using either bulk or CD8-enriched cultured cells as effectors, and either the autologous or HLA-mismatched B lymphocyte blasts uninfected or HSV-2 infected as targets. Effector/target cell ratio = 20:1. Bars: (a) 50 μm; (b) 10 μm.

intensity and better sensitivity than PE- (Fig. 2 c) or allophycocyanin-labeled (not depicted) tetramers bearing the same peptide.

Site-specific infiltration of HSV-2–specific CD8⁺ T cells in recurrent genital lesions

We first quantitated the number of total CD8⁺ cells in the lesional area during the acute stage of the herpetic lesion. Infiltrating CD8⁺ cells averaged 1,504 ± 337 cells/mm² in a 10-μm thick tissue ($n = 6$). Genital skin biopsies from 2 to 5 cm away ($n = 4$) revealed a dramatically decreased density of CD8⁺ cell infiltration (mean = 60 ± 48 cells/mm²), and skin biopsies of the arm region ($n = 4$) collected at the same time as the lesional biopsies averaged 12 ± 6 cells/mm² (Fig. 3 a). In addition, 30–50% of the CD8⁺ cells detected in both the distal arm area and neighboring genital skin were located within blood vessels, not in extravascular tissue. Thus, the CD8⁺ cell infiltration into dermal and epidermal skin tissue in persons with genital herpes lesions was limited spatially to the site of viral infection.

We then stained HSV-2–specific CD8⁺ T cells in situ by the Qdot 655–conjugated multimers during the acute lesional stage. In four out of the five patients tested, HSV-2–specific CD8⁺ T cells were detected in the epidermis, dermis, and dermal–epidermal junction of active lesions (Fig. 3 b) and were not visualized in either biopsies of distant skin or from areas 2–5 cm away from the active lesions. HSV-2–specific CD8⁺ T cells were not seen if Qdot multimers containing

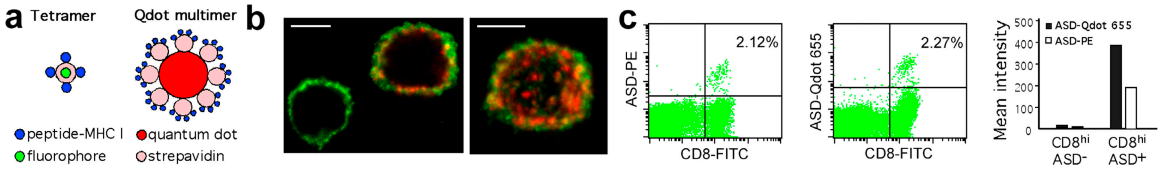

Figure 2. Qdot 655–conjugated peptide–MHC I multimer. (a) Schematic representation of the structure of Qdot 655–conjugated peptide–MHC I multimer complexes as compared with standard tetramers. (b) HSV-specific CD8⁺ T cells stained with an anti-CD8 antibody (green) and Qdot 655 multimer (red) for TCR recognizing the B*0702-restricted HSV-2 peptide gene *UL49* (aa 49–57). A maximum projection displays surface distributions of CD8 and TCR molecules on the double-positive cell (right). Stacks of confocal images were taken with a 100× objective at 0.2-μm intervals. (c) Detection of HSV-2–specific CD8⁺ T cells by flow cytometry using PE-labeled tetramer and Qdot 655–conjugated multimer. Peptide-stimulated (HSV-2 gene *UL46*, aa 354–362) PBMC from subject P1 was incubated either with A*0101/ASD-PE (left) or with A*0101/ASD–Qdot 655 (middle). Qdot multimer A*0101/ASD–Qdot 655 shows similar specificity but increased signal intensity as compared with PE-labeled tetramer (right). Bar, 5 μm.

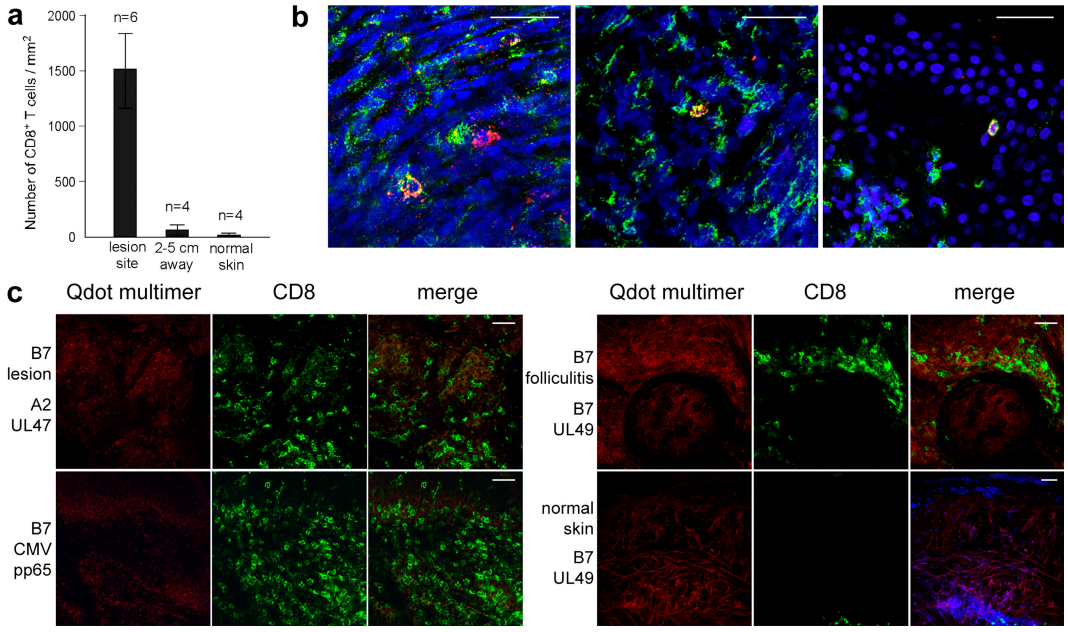

Figure 3. HSV-2–specific CD8$^+$ T cell infiltration in recurrent herpes lesion. (a) Quantitation of CD8$^+$ T cell infiltration in acute genital lesion compared with biopsies from adjacent normal genital skin or distal normal forearm skin. At least five fields were counted for each biopsy. (b) Detection of HSV-2–specific CD8$^+$ T cells in the epidermis (left), dermis (middle), and at the dermal–epidermal junction (right) in lesional skin. Biopsies were stained with anti-CD8 antibody (green), a cocktail of Qdot multimers (red), and DAPI (blue). HSV-2–specific CD8$^+$ T cells appear in yellow. (c) Absence of antigen-specific CD8$^+$ T cells in herpes lesions from the same patient using HLA-mismatched (left, top) or antigen-mismatched (left, bottom) Qdot multimers. HSV-2–specific CD8$^+$ T cells were also absent in folliculitis (right, top) or in normal skin (right, bottom), also in the same subject. Bars, 20 μm.

HSV-2 peptide combinations HLA-mismatched to the donor, or CMV pp65 peptide combinations HLA-matched to the donor, were used (Fig. 3 c). Additional specificity of the Qdot multimers for HSV-2 was demonstrated in subject P1, who developed a folliculitis in the genital skin during this study. Biopsy of the follicular lesion showed CD8$^+$ T cell infiltration (mean = 434 ± 24 cells/mm^2) but no evidence of HSV-2–specific CD8$^+$ T cells (Fig. 3 c).

The frequency of CD8$^+$ T cells specific for the HLA B*0702–restricted epitope *UL49* (aa 49–57) comprised ~10% of all CD8$^+$ cells in lesional tissue, ~100 times the frequency that these cells were found in blood (0.1% of CD8$^+$ cells). The enrichment of HSV-2–specific CD8$^+$ T cells in genital lesions was also seen in the two HLA A*0201–bearing subjects, where the frequency of detection was increased from undetectable in blood to 0.7 and 1.9% in tissues for subject P2 and P6, respectively (see Fig. 6 c). These data demonstrate that lesional CD8$^+$ T cells recognizing HSV-2 epitopes can be identified with a high degree of specificity using the Qdot multimer technique, that HSV-2–specific CD8$^+$ T cells home specifically to HSV-infected skin lesions, and that the CD8$^+$ T cell response to HSV-2 is highly focused anatomically.

Persistence of HSV-2–specific CD8 T cells after lesion resolution

To study the potential persistence of HSV-2–specific CD8$^+$ T cells after resolution of a herpetic lesion, subjects underwent repeated biopsies of the genital skin at the time of healing and sequential time periods from 2 to 8 wk after lesion resolution (Table I). The epidermis was intact and appeared clinically normal when these biopsies were taken. In contrast to acute infection, where HSV-2–specific CD8$^+$ T cells could be detected in all skin layers (Fig. 3 b), CD8$^+$ T cells in newly healed lesions were concentrated at the dermal–epidermal junction and in the upper dermis. HSV-2–specific CD8$^+$ T cells were detected in small clusters in the upper dermis, in particular just beneath the basement membrane, and very few CD8$^+$ cells infiltrated the epidermis (Video 4, available at http://www.jem.org/cgi/content/full/jem.20061792/DC1).

Resolution of the genital lesion was associated with skin reepithelialization and loss of HSV by culture or DNA detection in lesional biopsy tissue. However, HSV-2–specific CD8$^+$ T cells were consistently detected in healed genital skin along the dermal–epidermal junction. Most of the CD8$^+$ T cells, including HSV-2–specific CD8$^+$ T cells, were in close contact to basal keratinocytes (Fig. 4, a–c; and Video 5, available at http://www.jem.org/cgi/content/full/jem.20061792/DC1). This persistence of HSV-specific T cells at the dermal–epidermal junction in the lesional biopsies was documented in all of the postresolution biopsies of all six subjects studied. HSV-2–specific CD8$^+$ T cells persisted at similar frequencies to those in acute infection (see Fig. 6 c), suggesting that HSV-2–specific CD8$^+$ T cells remain locally enriched at the dermal–epidermal

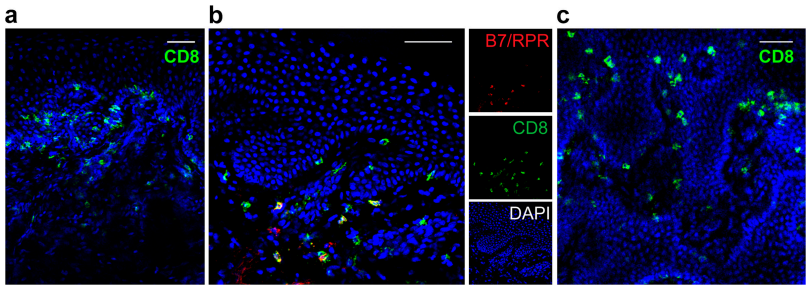

Figure 4. HSV-2–specific CD8$^+$ T cells persist at the dermal–epidermal junction after the lesion heals and reepithelializes. (a) Cross-sectional view of a biopsy taken 4 wk after healing. DAPI stain (blue) illustrates normal epidermal layer. CD8$^+$ T cells are found at the junction of the epidermis and dermis, and very few cells are located in the epidermis or in deep dermal areas. (b) Detection of HSV-2–specific CD8$^+$ T cells (yellow) at the dermal–epidermal junction in a biopsy taken 4 wk after healing. Tissue was stained with a cocktail of B*0702 *UL49*/RPR and *UL26*/GPH multimers (red) and anti-CD8 antibody (green). HSV-2–specific CD8$^+$ T cells appear in yellow. (c) A horizontal view demonstrates CD8$^+$ T cells in close contact with the basal cells at the basement membrane. The tissue was obtained from a skin biopsy of the original herpetic lesion area 4 wk after its clinical resolution. A similar pattern of CD8$^+$ T cells at the dermal–epidermal junction was seen in posthealing biopsies of all six subjects. Images represented here were from biopsies of subjects P1 (a and c) and P3 (b). Bars, 50 μm.

junction even in the wake of a waning overall inflammatory response.

Spatial relationship of CD8$^+$ T cells and cutaneous sensory nerve endings

Because HSV reactivates from cutaneous sensory nerve endings, we postulated that HSV-2–specific CD8$^+$ T cells persisting in healed genital herpes lesions would position themselves in close proximity to these nerves to optimally suppress reactivation. To test this hypothesis, we analyzed the spatial relationship between CD8$^+$ T cells and peripheral nerve endings. To visualize the three-dimensional topography of the cutaneous nerve plexus, we prepared dermal sheets, stained them with a monoclonal antibody against neural cell adhesion molecule (NCAM), and performed confocal microscopy. Free-ending nerve fibers and enveloped terminal Schwann cells formed a distinct network throughout the entire superficial dermis (Fig. 5 a). Nearly all the terminal nerve endings spread out within a thin layer below the dermal–epidermal junction, whereas large nerve trunks were located deeper in the dermis. In normal unaffected skin, CD8$^+$ cells were mainly detected in capillary blood vessels deep in the dermis and had no association with nerve-ending organs in the skin (Fig. 5 d and Fig. 3 c, normal skin). However, in posthealed lesional skin, many CD8$^+$ T cells were found adjacent to basal cells of the epidermis that were contacted by free nerve endings and adjacent to terminal Schwann cells (Fig. 5, b and c; and Video 6, available at http://www.jem.org/cgi/content/full/jem.20061792/DC1). We also documented CD8$^+$ T cells with HSV-2 specificity at these sites (Fig. 5 b). These findings showed that persisting CD8$^+$ T cells associate with sensory cutaneous nerve endings after lesion healing, often in the vicinity of basal keratinocytes, the primary infected cell type during reactivation of HSV. This spatial relationship suggests that HSV-specific CD8$^+$ T cells may control HSV reactivation peripherally by positioning themselves as sentinels at the interface between reactivating nerve endings and adjacent basal keratinocytes.

Relationship between HSV-2 detection in tissue and number and location of HSV-specific CD8$^+$ T cells

To investigate the temporal relationship between HSV-2 infection and CD8$^+$ T cell infiltration during and after genital herpes episodes, we subjected serial biopsies to viral DNA detection and CD8$^+$ T cell quantification. All 10 biopsies taken during acute lesions were both culture and PCR positive for HSV at the time of collection. For HSV-2 DNA, genome copies ranged from 2.2×10^3 to 5.4×10^6 per 50,000 cells (Fig. 6 a). HSV-2 DNA, as detected by PCR from tissue sections, rapidly decreased after healing (Fig. 6 a). Similarly, a rapid decrease in the number of CD8$^+$ T cells occurred during the course of healing (Fig. 6 b). All 31 biopsies done after reepithelialization, including 24 taken from the original lesion site and 7 taken from unaffected normal areas (4 adjacent to and 3 distal from the lesion), were cultured negative for HSV. 20 out of these 24 posthealing biopsies taken from the original lesion site and all 7 biopsies taken from unaffected sites were also negative for HSV-2 DNA.

Four posthealing lesional biopsies from two separate subjects demonstrated reappearance of HSV-2 DNA. Subject P2 had HSV-2 DNA detected in the 2-wk and the 8-wk posthealing biopsies (21 and 19 copies of HSV-2 DNA per 50,000 cells, respectively). No HSV-2 DNA was detected in the biopsies that preceded and followed the 8-wk biopsy. A similar pattern was seen in subject P3, who had HSV DNA detected at the 4-wk and 8-wk posthealing tissues (2 and 15 copies of HSV-2 DNA per 50,000 cells, respectively). Histologic sections of these skin biopsies showed an intact epithelium in all four of these biopsies; with no clinical or histologic evidence of ulceration or epidermal break (Fig. 6, d and e), as such, the HSV-2 shed into tissue was "subclinical" by definition.

Increased numbers of both HSV-2–specific and total CD8$^+$ T cells were detected in the posthealing biopsies in which HSV-2 DNA was present (Fig. 6, b–e). For example, the number of total CD8$^+$ T cells detected in the 8-wk

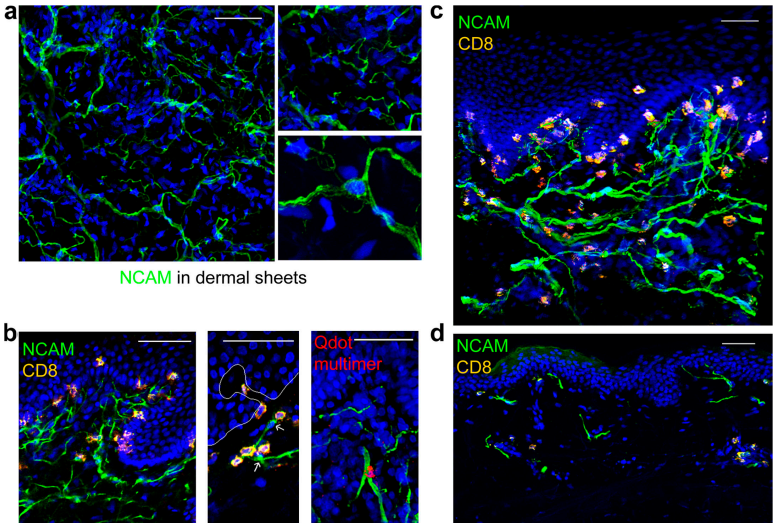

Figure 5. Spatial relationship between peripheral nerve endings and persisting CD8+ T cells in skin after healing. (a) Distribution of superficial nerve networks in dermal sheets. The dermal sheets were stained for NCAM (green) and counterstained with DAPI (blue). A projection of a 70-μm stack is shown from the top edge of the dermis (left). Free endings of nerve fibers (top) and terminal Schwann cells (bottom) are enlarged. (b) Close contact between CD8+ cells and cutaneous nerve endings. Biopsy tissue taken 4 wk after healing was double stained for CD8 (yellow) and NCAM (green). CD8+ cells are in close contact with the basal keratinocytes adjacent to free nerve endings at the basement membrane (left) and with terminal Schwann cells in the upper dermis (middle). A snapshot of a three-dimensional reconstruction (20-μm stack) displays spatial closeness between terminal nerve endings (green) and the cell with HSV-2 specificity (red; right). The tissue was from a biopsy taken 4 wk after healing and was stained with the A*0101/ASD and B*0702/RPR multimers and anti-NCAM antibody. (c) Similar findings are present in biopsy tissue 8 wk after healing. The snapshot shows a reconstructed three-dimensional distribution of CD8+ cells and cutaneous nerve endings. The image represents 25 μm in z. (d) Biopsy of normal skin of the upper arm was double stained for CD8 (yellow) and NCAM (green). Images represented were from biopsies of subjects P1 (b–d), P2 (b), and P6 (a). Bars, 50 μm.

posthealing biopsies for subjects P2 and P3, respectively, was 452 cells/mm^2 and 355 cells/mm^2, an average of four times higher than the two 8-wk biopsies from subject P1, who exhibited no detectable viral DNA after healing (104 cells/mm^2; Fig. 6 b). Subjects P2 and P3 possessed different HLA types, and hence, HSV-specific CD8+ T cells in the 8-wk biopsies were detected with different Qdot multimers, corroborating the specificity of the in situ detection of HSV-2–specific T cells during these episodes of subclinical HSV-2 reactivation (Fig. 6c-e). The association of CD8 infiltration with detection of HSV-2 DNA in the intact epidermis, in the absence of clinical symptoms, is most compatible with subclinical viral reactivation in which host containment of viral replication occurred before reactivated virus underwent extensive viral replication and disrupted the epithelial surface. These findings suggest that the HSV-2–specific CD8+ T cells at the site of genital herpes lesions contribute to local containment of viral replication.

DISCUSSION

One of the major questions in HSV-2 immunobiology has been the disparity between animal model data suggesting that functional host T cell responses in the ganglia have the ability to markedly limit viral reactivation at the ganglion level (25, 26) and human clinical studies of HSV-2 reactivation, which demonstrate that mucosal and genital skin shedding of HSV-2 in the immunocompetent person is extremely frequent (27–29). With once daily sampling, HSV-2 reactivation is seen in 20–60% of days in immunocompetent persons. More recent data suggest that high titer reactivations of HSV-2 lasting only 6–12 h are common (Mark, K., personal communication). These human clinical studies indicate that control of mucosal HSV-2 reactivation at the ganglion level in humans is incomplete at best. It is likely that immune control at both the ganglion and peripheral mucosal level is needed for containment of HSV reactivation. This study was designed to define whether local host control of HSV-2 played an important role in containing viral reactivation after lesional clearing. Our data indicate that much of the control of HSV-2 reactivation in humans appears to be consolidated in the peripheral mucosal immune compartment.

Our study indicates that the peripheral mucosal immune response to HSV-2 infection is highly concentrated both spatially and functionally. The cytolytic CD8+ T cell infiltration in genital herpes lesions is very specific to the site of infection. The dramatic reduction of CD8+ T cell density 2 cm outside of the affected skin-lesion area indicates that CD8+ T cell infiltration to an HSV infection is a very focused local event. The HSV-2–specific CD8+ T cells we detected were highly concentrated in the genital lesion. Quantitatively, HSV-2–specific T cells were present at 100 times higher concentrations in lesional skin than that in circulating blood. Even after lesion resolution, the enrichment

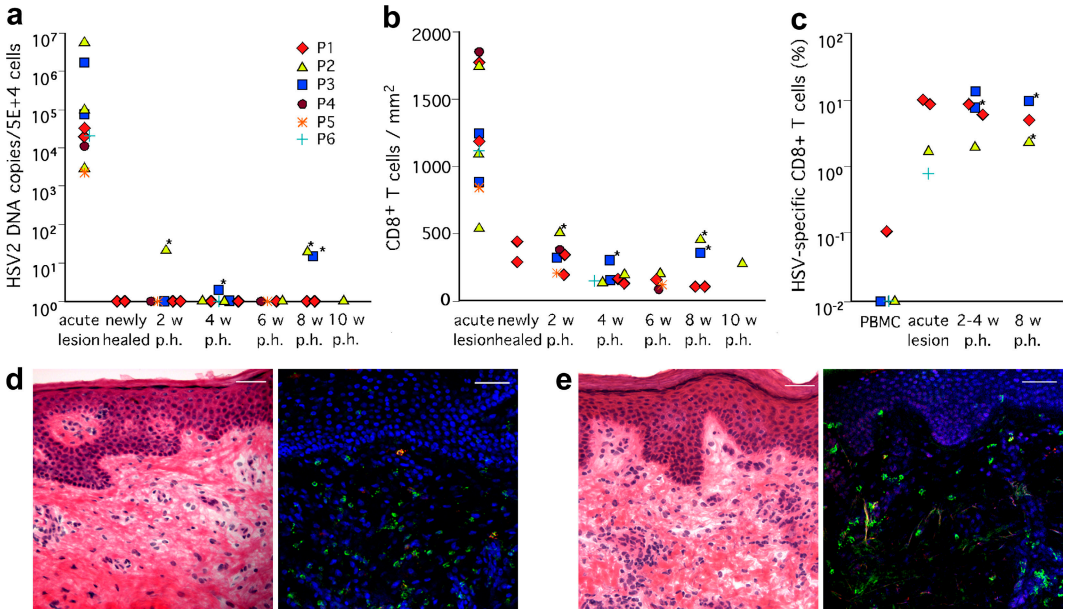

Figure 6. Subclinical reactivation of HSV-2 in genital skin is associated with increased CD8$^+$ T cell infiltration. (a–c) Quantitation of the HSV-2 genomic DNA (a), total CD8$^+$ T cells (b), and HSV-2–specific CD8$^+$ T cells (c) detected in skin biopsies. Each symbol represents one subject. HSV-2 DNA copies were quantitated by Taqman real-time PCR (see Materials and methods). Biopsies with reappearance of HSV-2 DNA after healing are marked with a star. (d and e) Hematoxylin and eosin and in situ staining of skin biopsies from subjects P2 (d) and P3 (e), in whom HSV-2 DNA was detected at 8 wk after healing. The epithelium is intact in both biopsies, and moderate lymphocyte infiltration is seen at the dermal–epidermal junction and in the dermis (left). In situ staining using a cocktail of A*0201 (d, right) and B*0702/RPR (e, right) Qdot multimer reveals that HSV-2–specific CD8$^+$ T cells are among the infiltrating CD8$^+$ cells in the dermis. Bars, 50 μm.

of HSV-2–specific CD8$^+$ T cells persisted in genital skin for an extended time period. Our study extended for only 2 mo, and local persistence was documented to last at least this long. Moreover, the spatial localization of HSV-2–persistent CD8$^+$ T cells appears to be of physiological importance. Unlike active lesions, where HSV-2–specific CD8$^+$ T cells were distributed in all layers of skin to eliminate viral infection and prevent spreading, HSV-2–specific CD8$^+$ T cells that persisted after healing were detected in the upper dermis and the dermal–epidermal junction, coincident with sensory nerve endings. This physical closeness between persistent CD8$^+$ T cells and sensory nerve endings would provide a potential mechanism in which the local immune system could quickly respond to and eliminate reactivated virus before it undergoes extensive replication. We demonstrated four such instances of such containment in two patients, as well as the apparent ability of host T cell responses in the periphery to contain viral reactivation before epithelial ulceration could occur.

Estimates of the frequency of HSV-specific CD8$^+$ T cells in genital skin are likely to be underestimates of their true prevalence in our studies. The cocktail of Qdot multimers we used was based on only a limited mapping of the breadth of the T cell response. As such, it is likely we were assaying only a portion of the CD8$^+$ T cell response to the virus. In more recent studies using a wider breadth of peptides, we have shown that many subjects possess CD8$^+$ T cells specific to a wider multitude of HSV proteins than we had available here (14). As such, our quantitative assessments are likely to be underestimates of the number of HSV-specific CD8$^+$ T cells in genital skin.

This study also provides evidence that HSV-specific CD8$^+$ T cells play a role in immune protection against clinically symptomatic HSV-2 reactivation in genital skin. The biopsies in which we detected HSV DNA in skin tissue, without evidence of epithelial cell destruction and in association with increased localized infiltration with HSV-2–specific CD8$^+$ T cells, suggest that resident HSV-2–specific T cells appear to be a critical component of cutaneous viral containment. The need to evolve a rapid response to viral replication in the desired region is emphasized by a clinical study, which showed that almost 40% of genital HSV-2 reactivation in humans were asymptomatic and lasted 6 h or less (Mark, K., personal communication). These short reactivations average from 10^3 to 10^4 copies of HSV-2 DNA per millimeter in swab specimens, indicating that prompt elimination of virus by the host mucosal immune responses occurred. Prospective studies investigating the relationship between in vivo persistence of HSV-2–specific T cells and the site and timing of clinical and subclinical reactivation are needed to define this association more closely. Although such studies require serial biopsies, patients with genital HSV-2 are affected greatly by this infection. The Qdot multimers and the in situ staining techniques we describe in this paper provide the tools for such studies to be undertaken.

In summary, HSV-2–specific $CD8^+$ T cells appear to play a direct role in viral clearance in vivo. These $CD8^+$ T cells migrate very specifically into genital lesions and persist preferentially in genital skin in the subepidermal layer contiguous to peripheral nerve endings, suggesting that they play a role in the earliest response to viral reactivation. Our studies indicate that persisting HSV-2–specific $CD8^+$ T cells function in immune surveillance and that the peripheral T cell response influences the frequency and clinical course of HSV-2 reactivation in humans.

MATERIALS AND METHODS

Human subjects and specimens. Six subjects (five female and one male) with recurrent genital HSV-2 infection and lesions were recruited into a study protocol approved by the University of Washington Institutional Review Board. All subjects were HIV-1/2 seronegative and had a history of culture-proven herpes disease. Serial 3-mm punch biopsies were obtained in subjects during an episode of symptomatic recurrence from the active lesion and at different stages thereafter (Table I). Lesional punch biopsies were taken from the erythematous skin immediately adjacent to a blister. After healing, punch biopsies were obtained from the site of the original lesion. In addition, 3-mm punch biopsies from an unaffected area 2–5 cm away from a lesion and/or the arm were also performed. Punch biopsies were divided into two halves: one half was snap frozen in optimum cutting temperature compound (Tissue-Tek; Sakura Finetek USA, Inc.) and stored at −80°C, whereas the other half was cut into three to four pieces and used immediately for immunofluorescence staining. Blood samples were drawn at the time of each biopsy.

In some biopsies, the epidermis and dermis were separated as described elsewhere (30). In brief, the subcutaneous tissue was removed with surgical scissors, and the remaining tissue was placed in cold PBS containing 5 mM EDTA and incubated at 4°C overnight. The epidermis was then dissected off the underlying dermis with a stereoscope (KL1500; Carl Zeiss MicroImaging, Inc.).

Synthesis of Qdot multimers. Peptide–MHC complexes (pMHCs) were formed in vitro as previously described (31). The HSV-2 peptides used were A*0101/ASD (*UL46*, aa 354–362), A*0201/FLI (*UL27*, aa 443–451), A*0201/FLV (*UL47*, aa 289–298), A*0201/GLA (*UL47*, aa 551–559), B*0702/RPR (*UL49*, aa 49–57), and B*0702/GPH (*UL26*, aa 475–483). The CMV peptide used was B*0702/NLV (*pp65*, aa 495–503). Streptavidin-coated Qdot 655 (Quantum Dot Corporation) was conjugated with a saturating amount of biotinylated pMHC on ice for 15 min and purified by gel filtration.

Immunofluorescence staining. Fresh tissue sections were stained overnight on ice in a casein solution (Vector Laboratories) with Qdot-conjugated MHC–peptide multimers (1:100), mouse anti–human CD8 (1:100; Caltag Laboratories), and rabbit anti–HSV-2 (1:500; DakoCytomation). Tissues were washed, fixed in 4% paraformaldehyde for 20 min at room temperature, and incubated with donkey anti–mouse Alexa Fluor 488 and donkey anti–rabbit Alexa Fluor 594 (1:100; Invitrogen) for 1 h at room temperature. After washing and incubating with DAPI (Fluka), tissue sections were mounted in Mowiol 40-88 containing 2.5% wt/vol DABCO (Sigma-Aldrich). Infiltrating $CD8^+$ T cells were enumerated in tissue fields of 460 × 460 μm in size, including the epidermis and 150–300 μm deep into the dermis. For calculating the median number of CD8 and HSV-specific $CD8^+$ T cells, at least five fields were counted for each biopsy. To calculate the percentage of HSV-2–specific $CD8^+$ T cells, Qdot multimer and CD8 double-positive cells were located, and total $CD8^+$ cells along those with HSV specificity were enumerated in tissue with a volume of 460 × 460 × 20 μm. For costaining of $CD8^+$ cells and nerve fibers, monoclonal CD8 Alexa Fluor 647 (1:100; Caltag Laboratories) and NCAM (1:50; Beckman Coulter) were used as primary antibodies, and donkey anti–mouse Alexa Fluor 488 was used as a secondary antibody.

Confocal microscopy. Confocal microscopy of immunofluorescence-labeled tissue was performed on a confocal microscope (LSM 510; Carl Zeiss MicroImaging, Inc.). For excitation of fluorescent dyes, the following laser lines were used: Alexa Fluor 488 and FITC, 488 nm; Alexa Fluor 594, 543 nm; Alexa Fluor 647, 633 nm; and Qdot 655, 458 nm. DAPI was excited in two-photon mode with a near-infrared laser (Chameleon; Coherent Inc.) tuned at 780 nm. The detection bands for the different dyes were as follows: Alexa Fluor 488 and FITC, 500–550 nm; Alexa Fluor 594, 565–615 nm; Alexa Fluor 647, 650–710 nm; Qdot 655, 650–710 nm; and DAPI, 435–485 nm. To minimize cross talk between dyes, imaging of multiple labeled samples was performed individually for each dye in a sequential mode. To reduce image noise, Kalman averaging (generally two to four frames) was used. For viewing of Qdot 655, a filter set with a 460-nm short-pass excitation filter, a 475-nm beam splitter, and a 635–675-nm band-pass emission filter was used (Chroma Technology Corp.). Three-dimensional rendering of confocal stacks was performed with Imaris (Bitplane AG) or Volocity (Improvision) software.

Flow cytometry. 5×10^6 PBMCs were incubated with Qdot 655–conjugated pMHC multimers for 15 min at room temperature. CD8-FITC antibody (Caltag Laboratories) was added, and cells were incubated for 30 min on ice, washed, and fixed. Acquisition was performed on a cytometer (LSR II; Becton Dickinson), and data were analyzed using CELLQuest software (Becton Dickinson). The detection limitation for HSV-2–specific $CD8^+$ T cells in PBMCs by flow cytometry was 0.01%.

Real-time quantitative PCR. DNA from skin biopsy samples was extracted using tissue kits (EZ1; QIAGEN). At least two sets of 60–80-μm thick cross-section tissues from each biopsy specimen were treated and followed previously described procedures for extraction and testing of HSV DNA (32, 33). Subtype-specific typing was performed by real-time PCR (34). The HSV DNA copy numbers were normalized to 50,000 cells by measuring the β-globin gene copy numbers using 5′-TGAAGGCTCATGGCAAGAAA-3′ and 5′-GCTCACTCAGTGTGGCAAAGG-3′ as primers and 5′-TCCAGGTGAGCCAGGCCATCACTA-3′ as a probe. The detection limitation of the assay was one copy per 50,000 cells.

Online supplemental material. Video 1 shows detection of $CD8^+$ cells in a genital herpes lesion. Video 2 provides a 180° view showing direct interaction between $CD8^+$ T cells and HSV-2–infected keratinocytes. Video 3 depicts the surface distribution of CD8 and TCR molecules on an HSV-2–specific $CD8^+$ T cell. Video 4 shows the distribution of $CD8^+$ and HSV-specific T cells in a newly healed genital herpes lesion. Video 5 provides a 360° display of persistent HSV-specific $CD8^+$ T cells in healed genital skin. Video 6 presents a 360° display of persistent HSV-specific $CD8^+$ T cells contiguous to cutaneous sensory nerve endings in healed genital skin. Online supplemental material is available at http://www.jem.org/cgi/content/full/jem.20061792/DC1.

We would like to thank David McDonald and Adrian Quintanilla for support with imaging; Christopher McClurkan, Alexis Klock, Khamsone Phasouk, and Hong Xie for technical assistance; Michael Remington and Steve Kuntz for clinical assistance; and Drs. David Myerson and Christopher Wilson for helpful discussions and suggestions.

This work was supported by National Institutes of Health grants AI-30731, AI-42528, AI-50132, and HD-051455.

The authors declare that they have no competing financial interests.

Submitted: 21 August 2006
Accepted: 30 January 2007

REFERENCES

1. Posavad, C.M., D.M. Koelle, M.F. Shaughnessy, and L. Corey. 1997. Severe genital herpes infections in HIV-infected individuals with impaired HSV-specific CD8+ cytotoxic T lymphocyte responses. *Proc. Natl. Acad. Sci. USA*. 94:10289–10294.

2. Koelle, D.M., and L. Corey. 2003. Recent progress in herpes simplex virus immunobiology and vaccine research. *Clin. Microbiol. Rev.* 16:96–113.
3. Augenbraun, M., J. Feldman, K. Chirgwin, J. Zenilman, L. Clarke, J. DeHovitz, S. Landesman, and H. Minkoff. 1995. Increased genital shedding of herpes simplex virus type 2 in HIV-seropositive women. *Ann. Intern. Med.* 123:845–847.
4. Khanna, K.M., R.H. Bonneau, P.R. Kinchington, and R.L. Hendricks. 2003. Herpes simplex virus-specific memory CD8(+) T cells are selectively activated and retained in latently infected sensory ganglia. *Immunity.* 18:593–603.
5. Liu, T., K.M. Khanna, X. Chen, D.J. Fink, and R.L. Hendricks. 2000. $CD8^+$ T cells can block herpes simplex virus type 1 (HSV-1) reactivation from latency in sensory neurons. *J. Exp. Med.* 191:1459–1466.
6. Cunningham, A.L., R.R. Turner, A.C. Miller, M.F. Para, and T.C. Merigan. 1985. Evolution of recurrent herpes simplex lesions: an immunohistologic study. *J. Clin. Invest.* 75:226–233.
7. Koelle, D.M., H. Abbo, A. Peck, K. Ziegweid, and L. Corey. 1994. Direct recovery of herpes simplex virus (HSV)-specific T lymphocyte clones from recurrent genital HSV-2 lesions. *J. Infect. Dis.* 169:956–961.
8. Koelle, D.M., H. Chen, M.A. Gavin, A. Wald, W.W. Kwok, and L. Corey. 2001. CD8 CTL from genital herpes simplex lesions: recognition of viral tegument and immediate early proteins and lysis of infected cutaneous cells. *J. Immunol.* 166:4049–4058.
9. Koelle, D.M., C.M. Posavad, G.R. Barnum, M.L. Johnson, J.M. Frank, and L. Corey. 1998. Clearance of HSV-2 from recurrent genital lesions correlates with infiltration of HSV-specific cytotoxic T lymphocytes. *J. Clin. Invest.* 101:1500–1508.
10. Haanen, J.B., M.G. van Oijen, F. Tirion, L.C. Oomen, A.M. Kruisbeek, F.A. Vyth-Dreese, and T.N. Schumacher. 2000. In situ detection of virus- and tumor-specific T-cell immunity. *Nat. Med.* 6:1056–1060.
11. Skinner, P.J., M.A. Daniels, C.S. Schmidt, S.C. Jameson, and A.T. Haase. 2000. Cutting edge: In situ tetramer staining of antigen-specific T cells in tissues. *J. Immunol.* 165:613–617.
12. Schmitz, J.E., R.S. Veazey, M.J. Kuroda, D.B. Levy, A. Seth, K.G. Mansfield, C.E. Nickerson, M.A. Lifton, X. Alvarez, A.A. Lackner, and N.L. Letvin. 2001. Simian immunodeficiency virus (SIV)-specific cytotoxic T lymphocytes in gastrointestinal tissues of chronically SIV-infected rhesus monkeys. *Blood.* 98:3757–3761.
13. McGavern, D.B., U. Christen, and M.B. Oldstone. 2002. Molecular anatomy of antigen-specific CD8(+) T cell engagement and synapse formation in vivo. *Nat. Immunol.* 3:918–925.
14. Hosken, N., P. McGowan, A. Meier, D.M. Koelle, P. Sleath, F. Wegener, M. Elliott, L. Grabstein, C. Posavad, and L. Corey. 2006. Diversity of the CD8+ T cell response to herpes simpolex virus type 2 proteins among persons with genital herpes. *J. Virol.* 80:5509–5515.
15. McMichael, A.J., and S.L. Rowland-Jones. 2001. Cellular immune responses to HIV. *Nature.* 410:980–987.
16. Hislop, A.D., N.H. Gudgeon, M.F. Callan, C. Fazou, H. Hasegawa, M. Salmon, and A.B. Rickinson. 2001. EBV-specific CD8+ T cell memory: relationships between epitope specificity, cell phenotype, and immediate effector function. *J. Immunol.* 167:2019–2029.
17. Fellner, M. 1976. Green autoflurescence in human epidermal cells. *Arch. Dermatol.* 112:667–670.
18. Zeng, H., C. MacAulay, D.I. McLean, and B. Palcic. 1995. Spectroscopic and microscopic characteristics of human skin autofluorescence emission. *Photochem. Photobiol.* 61:639–645.
19. Na, R., I.M. Stender, M. Henriksen, and H.C. Wulf. 2001. Autofluorescence of human skin is age-related after correction for skin pigmentation and redness. *J. Invest. Dermatol.* 116:536–540.
20. Bruchez, M., Jr., M. Moronne, P. Gin, S. Weiss, and A.P. Alivisatos. 1998. Semiconductor nanocrystals as fluorescent biological labels. *Science.* 281:2013–2016.
21. Pinaud, F., X. Michalet, L.A. Bentolila, J.M. Tsay, S. Doose, J.J. Li, G. Iyer, and S. Weiss. 2006. Advances in fluorescence imaging with quantum dot bio-probes. *Biomaterials.* 27:1679–1687.
22. Wu, X., H. Liu, J. Liu, K.N. Haley, J.A. Treadway, J.P. Larson, N. Ge, F. Peale, and M.P. Bruchez. 2003. Immunofluorescent labeling of cancer marker Her2 and other cellular targets with semiconductor quantum dots. *Nat. Biotechnol.* 21:41–46.
23. Chattopadhyay, P.K., D.A. Price, T.F. Harper, M.R. Betts, J. Yu, E. Gostick, S.P. Perfetto, P. Goepfert, R.A. Koup, S.C. De Rosa, et al. 2006. Quantum dot semiconductor nanocrystals for immunophenotyping by polychromatic flow cytometry. *Nat. Med.* 12:972–977.
24. Koelle, D.M., Z. Liu, C.L. McClurkan, R.C. Cevallos, J. Vieira, N.A. Hosken, C.A. Meseda, D.C. Snow, A. Wald, and L. Corey. 2003. Immunodominance among herpes simplex virus-specific CD8 T-cells expressing a tissue-specific homing receptor. *Proc. Natl. Acad. Sci. USA.* 100:12899–12904.
25. Khanna, K.M., A.J. Lepisto, V. Decman, and R.L. Hendricks. 2004. Immune control of herpes simplex virus during latency. *Curr. Opin. Immunol.* 16:463–469.
26. Prabhakaran, K., B.S. Sheridan, P.R. Kinchington, K.M. Khanna, V. Decman, K. Lathrop, and R.L. Hendricks. 2005. Sensory neurons regulate the effector functions of CD8(+) T cells in controlling HSV-1 latency ex vivo. *Immunity.* 23:515–525.
27. Wald, A., L. Corey, R. Cone, A. Hobson, G. Davis, and J. Zeh. 1997. Frequent genital herpes simplex virus 2 shedding in immunocompetent women: effect of acyclovir treatment. *J. Clin. Invest.* 99:1092–1097.
28. Wald, A., J. Zeh, S. Selke, T. Warren, A.J. Ryncarz, R. Ashley, J.N. Krieger, and L. Corey. 2000. Reactivation of genital herpes simplex virus type 2 infection in asymptomatic seropositive persons. *N. Engl. J. Med.* 342:844–850.
29. Gupta, R., A. Wald, E. Krantz, S. Selke, T. Warren, M. Vargas-Cortes, G. Miller, and L. Corey. 2004. Valacyclovir and acyclovir for suppression of shedding of herpes simplex virus in the genital tract. *J. Infect. Dis.* 190:1374–1381.
30. Tschachler, E., C.M. Reinisch, C. Mayer, K. Paiha, H. Lassmann, and W. Weninger. 2004. Sheet preparations expose the dermal nerve plexus of human skin and render the dermal nerve end organ accessible to extensive analysis. *J. Invest. Dermatol.* 122:177–182.
31. Altman, J.D., P.A. Moss, P.J. Goulder, D.H. Barouch, M.G. McHeyzer-Williams, J.I. Bell, A.J. McMichael, and M.M. Davis. 1996. Phenotypic analysis of antigen-specific T lymphocytes. *Science.* 274:94–96.
32. Magaret, A.S., A. Wald, M.L. Huang, S. Selke, and L. Corey. 2007. Optimizing PCR positivity criterion for detection of HSV DNA on skin and mucosa. *J. Clin. Microbiol.* In press.
33. Wald, A., M.L. Huang, D. Carrell, S. Selke, and L. Corey. 2003. Polymerase chain reaction for detection of herpes simplex virus (HSV) DNA on mucosal surfaces: comparison with HSV isolation in cell culture. *J. Infect. Dis.* 188:1345–1351.
34. Corey, L., M.L. Huang, S. Selke, and A. Wald. 2005. Differentiation of herpes simplex virus types 1 and 2 in clinical samples by a real-time taqman PCR assay. *J. Med. Virol.* 76:350–355.